Protocol for Segmentation of the Human Hippocampus, Entorhinal Cortex, Perirhinal Cortex, and Parahippocampal Cortex

John B. Pluta, Laura E.M. Wisse, Long Xie, Dave A. Wolk, Paul A. Yushkevich

9/3/2016

Introduction

This document describes the protocol for manual segmentation of the hippocampal formation (HF) and surrounding extrahippocampal medial temporal lobe (MTL) structures. The initial version of this protocol, restricted to labeling several MRI slices in the body of the HF, was described in (Yushkevich et al., 2010) and derived from (Mueller et al., 2007). The primary differences with protocol in (Mueller et al., 2007) were the separate labeling of the cornu ammonis 3 (CA3) subfield, which is grouped with dentate gyrus (DG) by Mueller et al. (2007), and expansion to a greater number of body slices (4-6 slices compared to 3 labeled by Mueller et al. (2007)). In (Yushkevich et al., 2014), we extended our protocol to label subfields in the anterior ("head") and posterior ("tail") portions of the HF, with rules for subfield differentiation based on other full-length HF segmentation protocols (Malykhin et al., 2010; Wisse et al., 2012). The underlying anatomical reference for the protocol was described in (Duvernoy, 2005), but to gain greater understanding of underlying anatomical variability, we also consulted a library of 25 high-resolution postmortem MRI scans of the intact HF obtained as described in (Yushkevich et al., 2009). The protocol also provided more detailed labeling of extrahippocampal regions than (Yushkevich et al., 2010). In addition to the entorhinal cortex (ERC), the protocol included the perirhinal cortex (PRC), which is further partitioned into Brodmann areas 35 and 36 (BA35 and BA36). While these structures begin at the rostral end of the temporal lobe, their shape and appearance is more regularly well defined around the HF. Thus we segmented only the caudal aspect of these cortices, beginning one slice anterior to the hippocampal head and ending one slice posterior. The protocol for labeling ERC and PRC was derived by adapting the protocol in (Ding & Van Hoesen, 2010) to *in vivo* MRI data, with extensive input from the first author of that protocol. The revision of the protocol in this study has been further extended to include the posterior portion of the parahippocampal cortex (PHC), based on (Kivisaari et al., 2013), and occipito-temporal sulcus (OTS).

This protocol defines three macroscopic subregions (head, body, and tail), in the HF, and describes the labeling of each region in separate sections. A final section describes the labeling of the MTL regions.

1

Images

This protocol is applicable to images obtained using an imaging sequence similar to that described in (Mueller et al., 2007). Specifically, sequences of this class acquire coronal slices of the brain angled orthogonally to the long axis of the hippocampus, with very high in-plane resolution and low out-of-plane resolution (typically, 0.5mm x 0.5mm or smaller in-plane, and 1.0-3.5mm out-of-plane). The images are T2-weighted to allow for the visualization of certain neuronal layers in the hippocampus. Particularly, a hypointense band, typically 1-2 pixels thick, is reliably observed in the hippocampus proper in these scans. This band encompasses strata radiatum, lacunosum and moleculare of the cornu ammonis (CA); the stratum moleculare of the DG. This hypointense band serves as the primary visual feature for delineating the DG from the CA through the entire length of the HF. We adopt the nomenclature in (Kerchner et al., 2010), and refer to this hypointense band as the SRLM for short. Arrows in Figure 1 identify the SRLM in example head, body, and tail slices. In images where the SRLM is not visible, e.g. due to MRI artifact or severe neurodegeneration, HF subfield segmentation cannot be performed.

Table 1. Labeling color scheme for hippocampal formation subfields and medial temporal lobe regions, and the regions of the hippocampal formation in which the subfields are labeled.

| Color	Anatomical Region	Extent
	CA1	Head, Body, Tail
	CA2	Head (Partial), Body
	CA3	Head (Partial), Body
	DG	Head, Body, Tail
	Subiculum	Head, Body
	ERC	Head, 1 Body Slice
	PRC (BA 35)	Head, 2 Body Slices
	PRC (BA 36)	Head, 2 Body Slices
	PHC	
	CS	
	OTS	
	Cerebrospinal Fluid	Head, Body, Tail
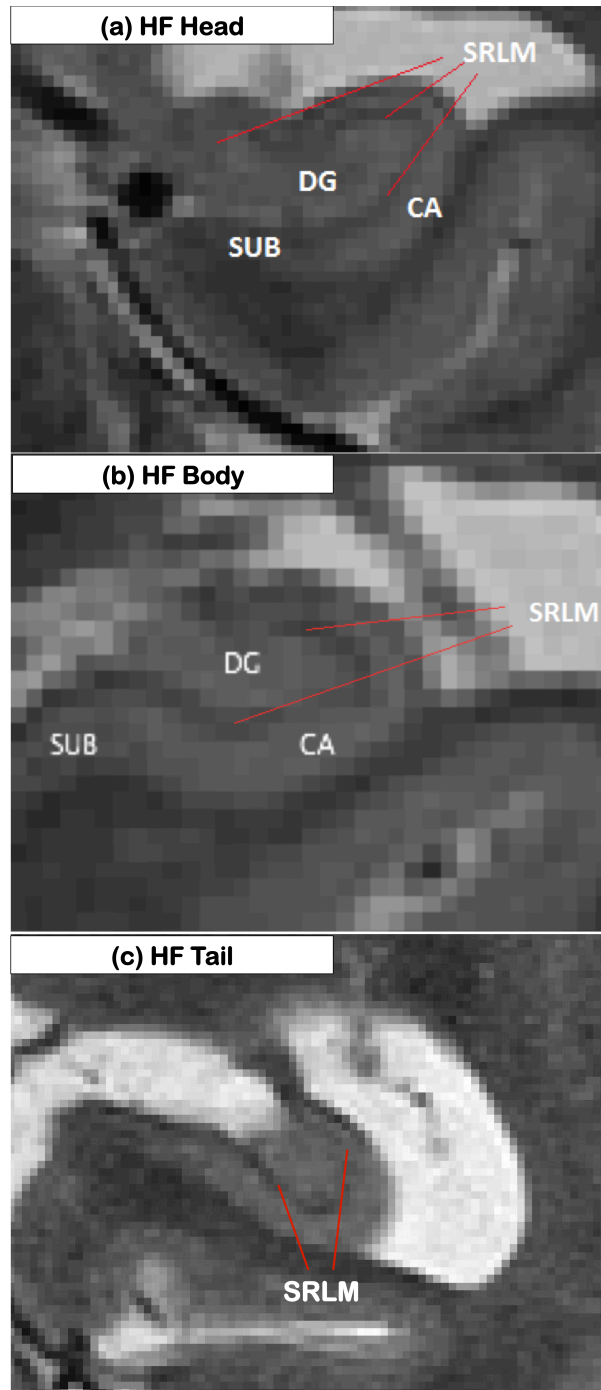
Figure 1. SRLM in a hippocampal formation (HF) head (a), body (b) and tail (c) slices.

ITK-SNAP

Images are segmented using polygon drawing and paintbrush interaction modes in ITK-SNAP software, which allows simultaneous labeling of 3D image volumes in three orthogonal slice views (Yushkevich et al., 2006). Given the anisotropic nature

of the T2-weighted MRI images, labeling is done primarily in the coronal slice, but sagittal and axial slices, as well as the 3D rendering[1] of the segmentation, are monitored to ensure three-dimensional continuity of the segmentation. The protocol also takes advantage of the annotation tools in ITK-SNAP.
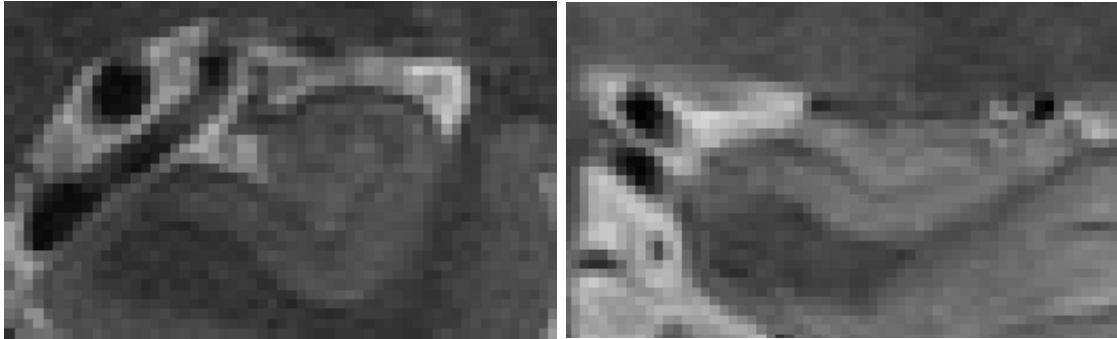

Figure 2. Various shapes of the hippocampal formation body.

Segmentation of Hippocampal Sections

Body

In the body of the HF, DG is mostly interior, with CA wrapping around it in a "swiss-roll" shape, though there is substantial variability in the appearance of body sections between subjects (Figure 2). CA and DG are separated by the SLRM (see Figure 1b), and slices in the body look similar to one another. DG is bounded laterally and inferiorly by the SLRM, and bounded medially by cerebrospinal fluid (CSF). In the superior direction, the SLRM bounds the interior portion of DG, while the exterior is bounded by the Fimbria (Figure 3a), which also appears as hypointense voxels. CA enters into DG in the superior extent. While the true transition between CA3 and CA4 occurs within the DG and is not visible at this resolution, thus a heuristic estimate is used. The voxels of the immediate entry point of CA are considered CA3 (that is, penetrating one voxel deep into DG), as are adjacent voxels in the superior direction, extending one voxel superior to DG.
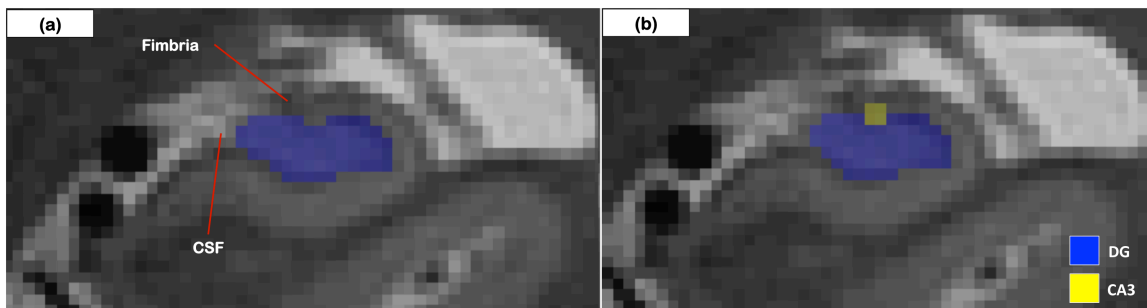

Figure 3. A typical body slice with DG (a), DG and CA3 (b)

---

[1] Due to the small size of some subfields and the anisotropy of the images, the default ITK-SNAP settings are modified to disable Gaussian smoothing during 3D rendering.

4

The SRLM is not given its own label because it is often less than one voxel wide due to partial volume effects. It is generally assigned to DG, unless the SRLM is two or more voxels wide, in which case it is evenly split between DG and CA. Figure 3a has an illustration of the example subject with DG segmented. The medial extent of CA is segmented as CA3, and extends one voxel above the most superior point of the adjacent DG. Most of CA3 is inside DG and the two are indistinguishable, and this method is only a crude approximation. Figure 3b illustrates the example body slices with CA3 segmented.

As shown in Figure 4, CA2 is segmented by drawing a line from the medial edge of CA3 to the lateral edge of DG. Then a second line is drawn orthogonal to the first at its mid-point. The medial boundary of CA2 is CA3, and the lateral boundary is one voxel past the vertical line. As a typical T2 sequence lacks the resolution to capture the anatomical features defining CA2, this heuristic rule is used as an approximation.
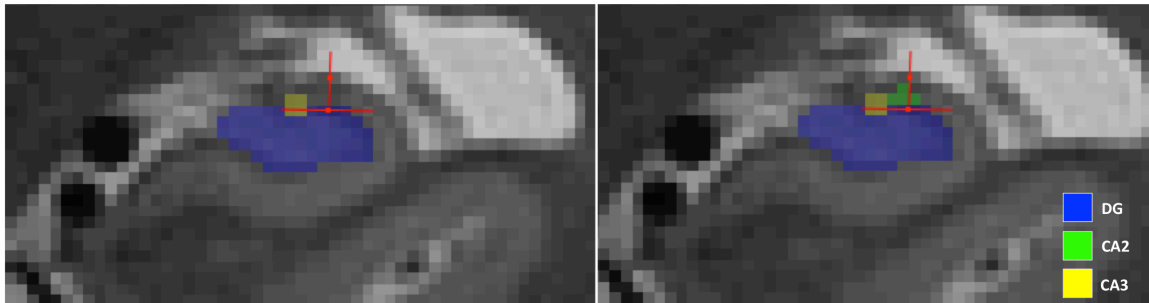
Figure 4. Process for delineating CA2 in the body. CA2 boundary is defined relative to CA3 and the lateral edge of DG.

CA1 extends from end of CA2 to the most medial point of DG. Since the shape of DG may determine the orientation of CA, capturing the curvature of CA is necessary for anatomically sensible estimates. Thus, a line is drawn along the inferior-medial edge of DG, and another line is drawn orthogonal to this at the CA/DG boundary. This edge forms the CA1/subiculum (SUB) boundary. This method likely includes a small part of SUB towards CA1, however it is necessary to ensure consistency, as the actual CA1/SUB transition is gradual and not observable at this resolution. Finally, the SUB is segmented from the edge of CA1 to the most medial point of the cortex. This protocol draws no distinction between presubiculum and SUB. This process is shown in Figure 5.
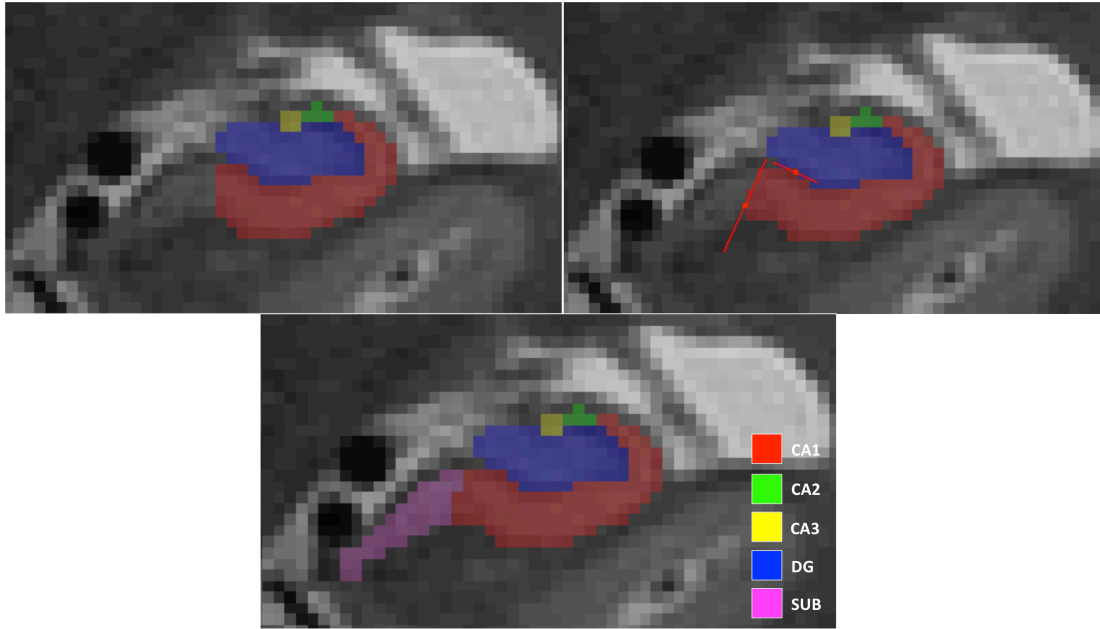
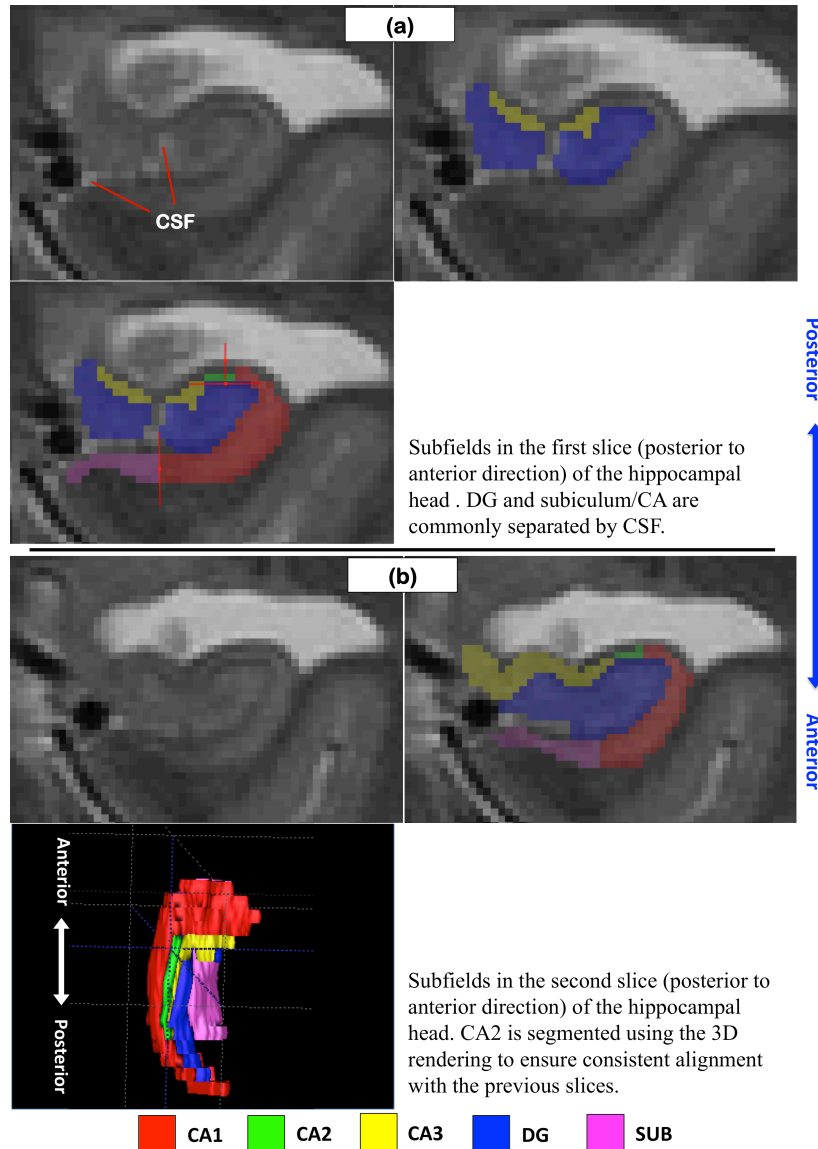**Figure 5**. CA1-3, DG, SUB in a body slice.

Head

Unlike the relatively homogenous body, the head of the hippocampus is a complex region with a great deal of variety in the appearance of each slice (Figure 2). As in the body (Figure 1a), segmentation depends on the dark band being visible to separate DG and CA, with further heuristic rules for defining the CA subdivisions and the SUB. In this protocol, the head is defined as beginning in the first slice where the uncal apex is visible. The uncus is a complex transitional region consisting of CA3 and DG. In the posterior extent, it is entirely CA3, and quickly transitions into mostly DG.
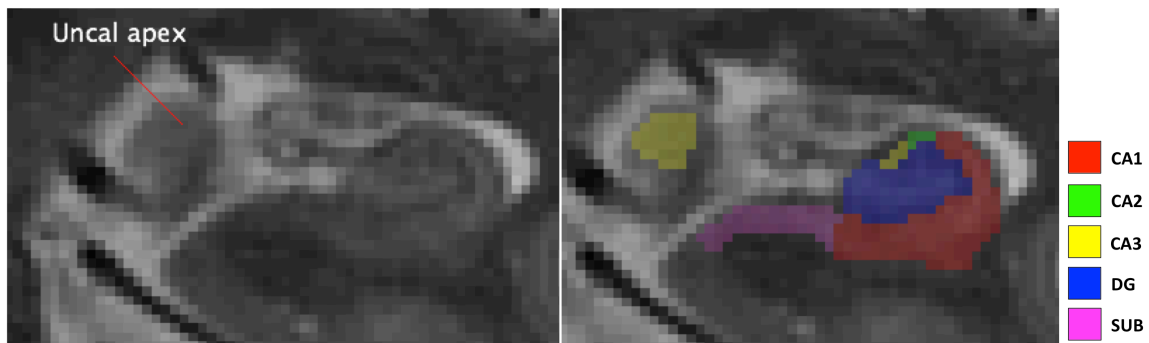
**Figure 6.** Uncal apex in posterior extent of the hippocampal formation head.

Typically, the uncus and hippocampal body will be two discrete sections in the first (most posterior) head slice, either the apex of the uncus (Figure 6) or a more anterior section of the uncus (Figure 7a). In this case, the body is segmented essentially as normal, though CA3 will extend more medially. CA3 still extends one voxel

above the adjacent DG, and the most medial point of CA3 on this line (as opposed to the entire body section) is used to determine the boundary for CA2, following the same rules as in the body. Similarly, the CA1/SUB boundary is determined the same way as in the body as well.

Subfields in the first slice (posterior to anterior direction) of the hippocampal head . DG and subiculum/CA are commonly separated by CSF.

Subfields in the second slice (posterior to anterior direction) of the hippocampal head. CA2 is segmented using the 3D rendering to ensure consistent alignment with the previous slices.

CA1   CA2   CA3   DG   SUB

Figure 7. Subfields in the first two slices (posterior to anterior direction) of the hippocampal head. Blue arrow indicates the relative position of the two slices.

Where DG is mostly interior throughout the hippocampus, the uncal and head region has a significant exterior projection (see Figure 8). Thus most of the uncal section is composed of DG, with a small band of CA3 that is separable by either the presence of the dark band or more subtle intensity changes. It should be roughly the same width as CA3 in the body (Figure 7a).
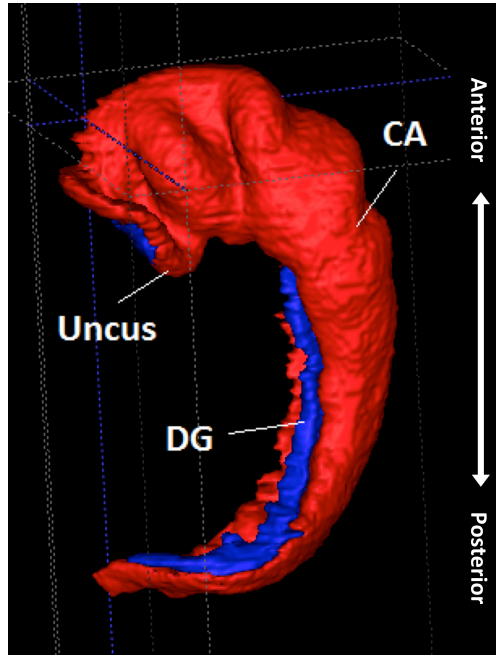
Figure 8. 3D representation of the CA and DG subfields in the hippocampal formation. The apex of the uncal region indicates the beginning of the hippocampal head. White arrow indicates the anterior-posterior direction.

Continuing in the anterior direction, the DG projection ends and instead, CA projects. The superior CA portion in this slice is a complicated region that transitions between the CA1, CA2, and CA3 subfields in both the medial-lateral and anterior-posterior axes. However, there are no macroscopic features identifying these specific changes, so only an estimate is possible. The majority of the superior length of CA is comprised of CA3, thus CA2 and any medial part of CA1 are all grouped under this label, up to the most superior point of DG. As the shape of the head is quite variable, geometric rules do not apply. Thus, the CA2 label in this section is guided by the position of CA2 in the previous slices. The 3D view is used to segment CA2 in a position consistent with the rest of the labels (see Figure 7b).

Segmentation of CA3 in the head stops when digitations in the head appear, shown in Figure 9, which in a typical dataset will be 1-3 slices (though this depends on slice thickness). In most subjects, there will be two head slices with CA3; a slice with the uncus, and the next anterior slice. In subjects where the uncal apex is visible, there may be as many as 3 slices (including the apex).
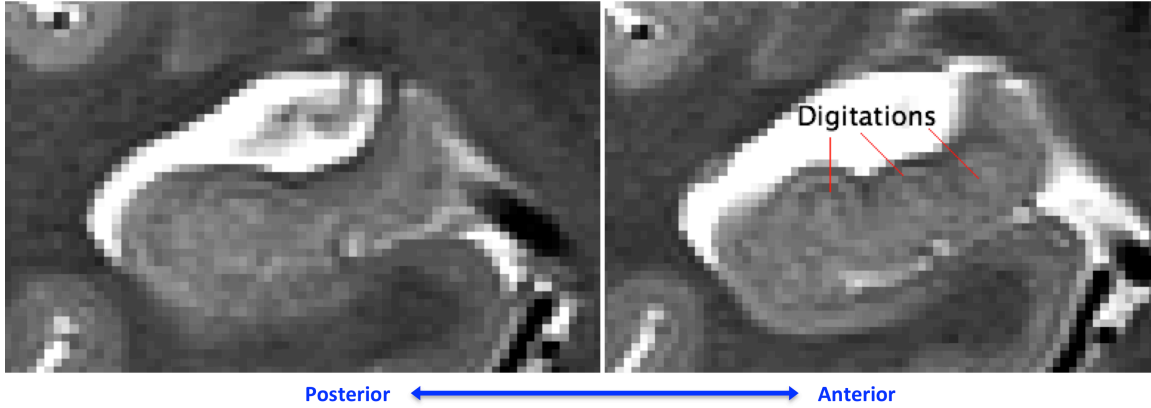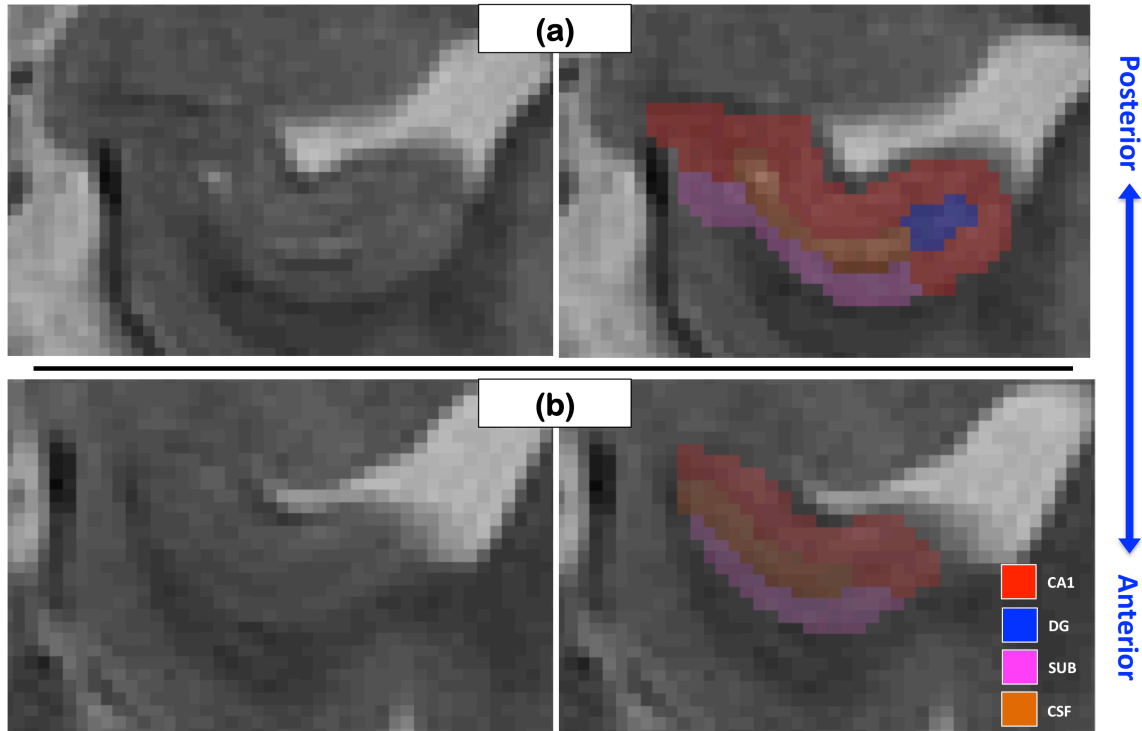
Figure 9. Digitations in the hippocampal formation head indicate the anterior boundary of the CA3 region. Blue arrow indicates the relative position of the two slices.

Subsequent head slices (Figure 10) are labeled as CA1 and DG, separated by the SRLM. SUB boundaries in these slices are determined with a method similar to that described in (Wisse et al., 2012), by simply using the same voxel location; the cross-hair tool can be used slice to slice to ensure that the position is the same. This same position is retained for the rest of the slices of the head, with a proportionately greater amount of SUB in more anterior slices.


Posterior ⟵ ⟶ Anterior
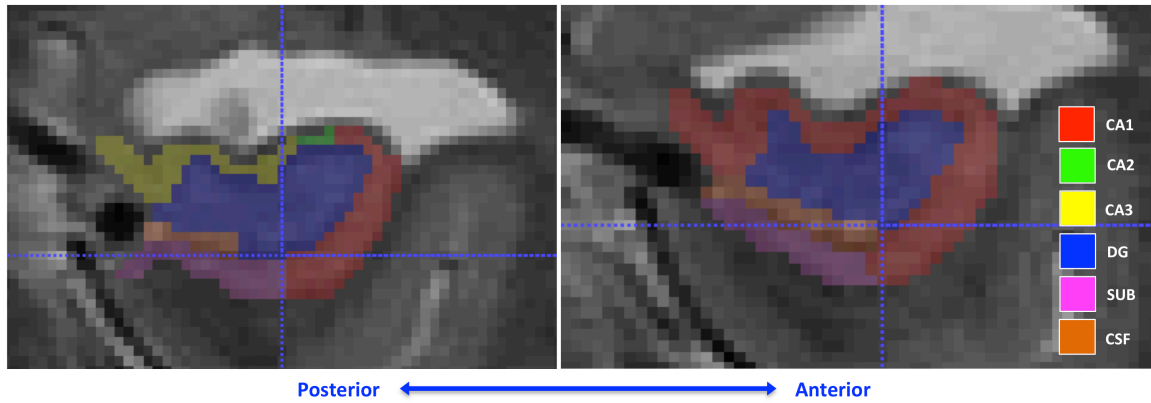
Figure 10. Two consecutive slices in the anterior direction of the hippocampal head. The crosshairs remain in the same physical location, slice to slice, to determine the CA1/SUB boundary in the hippocampal head. Blue arrow indicates the relative position of the two slices.

Figure 11. Two consecutive slices of the hippocampal formation head in the anterior direction. The slice in the bottom row is more anterior than the slice in the top row. The anterior aspect of the head is mostly comprised of CA1 and SUB, often separated by a region of CSF. Blue arrow indicates the relative position of the two slices.

More anterior slices have progressively less DG present, with the most anterior slices being entirely CA and SUB, which are separated by CSF (Figure 11). The hippocampus ends in the anterior direction when the head is no longer visible. Some tissue may still be visible though partially volumed or otherwise ambiguous. If the slice cannot be clearly segmented, it is not included as part of the hippocampus (Figure 12).
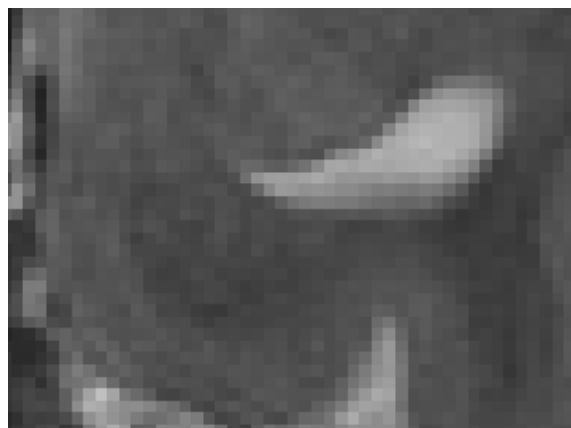
Figure 12. Anterior slice showing ERC and PRC, but the hippocampus is no longer visible.
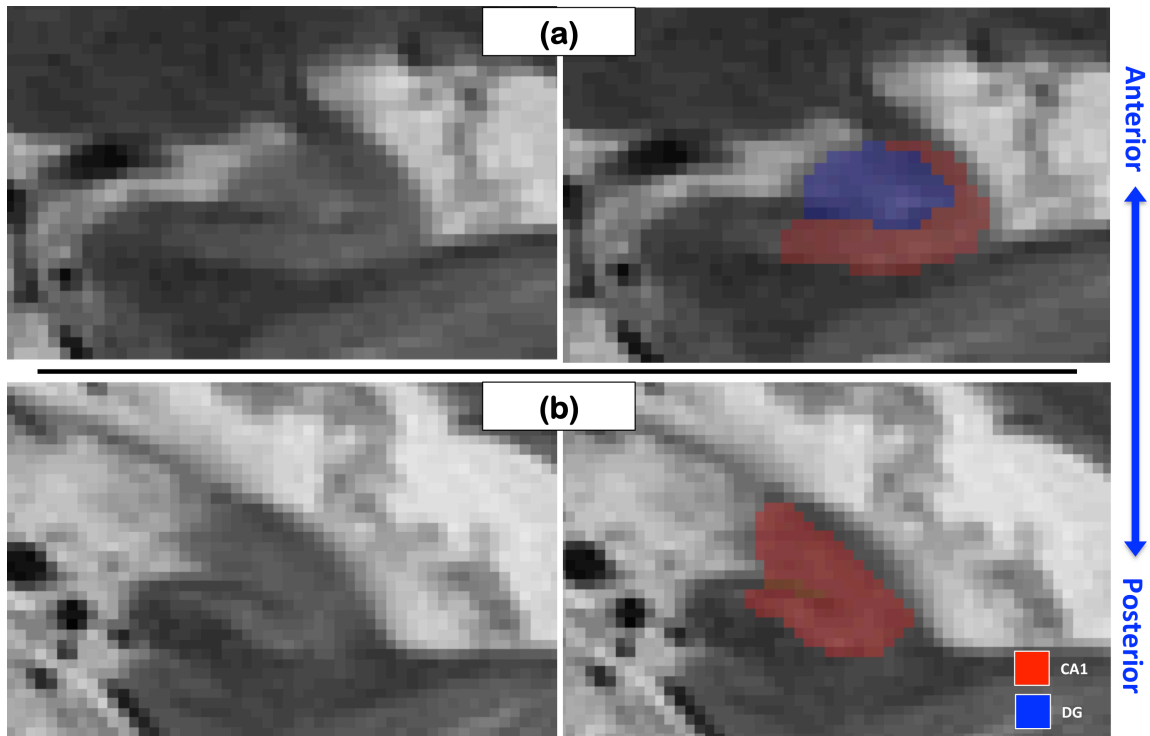
Tail

The body to tail transition is more ambiguous than body to head. It is generally noted by observing a change in the shape of the hippocampal body, with more digitation in CA and a more oblong shape in DG. One possible proxy for the hippocampal tail is the appearance of the wing of the ambient cistern (AC; see Figure 13). In this protocol, the wing of the ambient cistern is used as a general guideline, and final determination of a slice's classification as belonging to the hippocampal tail is determined by its shape.
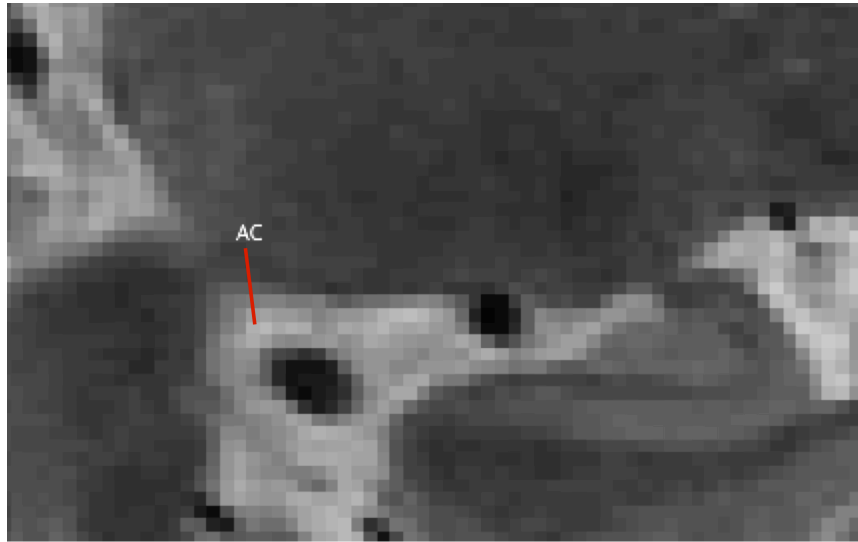
Figure 13. Wing of the ambient cistern (AC).

Because of the change in shape and other anatomical features, segmenting the CA subfields is difficult in the tail. Thus, only CA1 and DG are segmented with CA2/3 grouped into CA1, separated by the dark band as usual (Figure 14a). SUB is not included. Labeling continues in the posterior direction until DG and CA1 can longer be separated. This slice is segmented entirely as CA1; though it likely contains DG tissue, it is mostly CA and the two are inseparable at this resolution (Figure 14b). The first slice to be segmented as entirely CA1 is also considered to be the posterior extent of the hippocampus.

Figure 14. Segmentation of a typical tail slice (a) and a slice of the posterior extent of the hippocampal tail (b). Blue arrow indicates the relative position of the two slices.

Segmentation of Extrahippocampal Structures

Entorhinal Cortex (ERC)

In this protocol, the ERC is segmented in a limited region extending from one slice past the anterior boundary of the hippocampal head, to one slice past the uncal apex. Segmentation is limited in the caudal region of ERC because it has an indistinct appearance from surrounding cortical tissue in its most rostral aspect. The anterior boundary is chosen because the ERC is well defined in the region around the hippocampal head. The posterior boundary is chosen to approximate the anatomical border displayed in (Insausti et al., 1998).

Within a coronal slice, the ERC occupies the medial bank of the collateral sulcus, and is both histologically and macroscopically distinct (slightly hypointense) from the surrounding cortical tissue and hippocampus. It is possible to segment ERC based solely on image intensity and appearance, with guidance provided by figures in (Insausti et al., 1998) and (Ding et al., 2009). Figures 15-17 give examples of the ERC in MR images.

Perirhinal Cortex (PRC)

Although the PRC extends to well beyond the hippocampus in towards the caudal end of the temporal pole, it is difficult to consistently segment it for reasons similar to those mentioned in the ERC section. Thus, the same anterior boundary is used (one slice anterior of the end of the hippocampal head). In the posterior direction, the ERC is posterior to the uncal apex (Insausti et al., 1998), and PRC ends one slice posterior to this. In these most posterior slices, PRC wraps around and encapsulates ERC. Thus the entire medial bank consists of BA35 (instead of ERC as in previous slices), as illustrated in Figure 15. Figure 5 in (Insausti et al., 1998) provides an example of the anterior and posterior bounds of PRC.

| | CA1 | | CA2 | | CA3 | | DG | | SUB | | CSF | | ERC | | BA35 | | BA36 | | CS | | OTS |
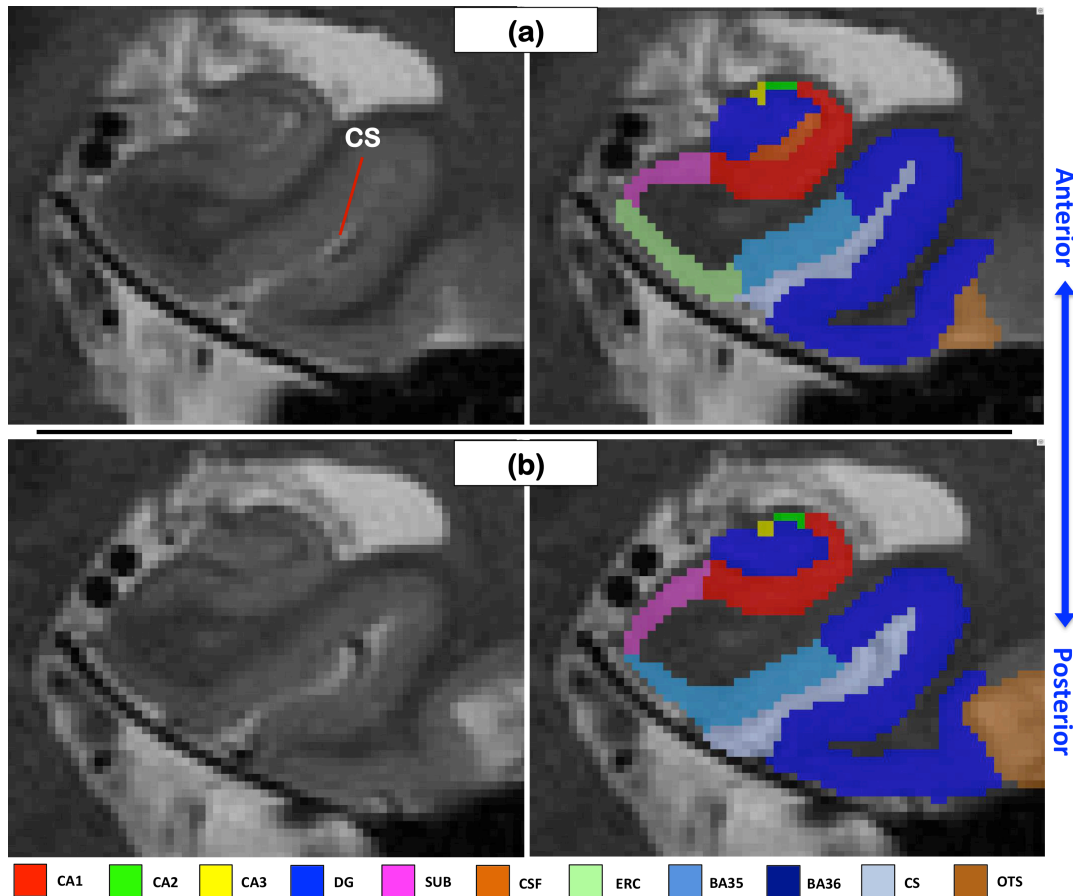
Figure 15. Transition from the most posterior slice of ERC (a) to the most posterior slice of PRC (b). PRC wraps around and covers over ERC, such that the last slice is composed entirely of PRC. Blue arrow indicates the relative position of the two slices.

Within a slice, segmentation of the PRC and it's substructures is based on the definitions in (Ding & Van Hoesen, 2010), which are considerably different than those proposed in (Insausti et al., 1998). The discussion section of (Ding & Van Hoesen, 2010) addresses the discrepancies between the two papers. The PRC is composed of two distinct sections, defined as BA35 and BA36. Boundaries for both

substructures depend of the shape and appearance of the sulci in that region, particularly the CS and the OTS. In general, BA35 occupies the medial bank of the CS, and is slightly thicker than BA36 due to the presence of an extra neuronal layer that is unique to this region (Ding & Van Hoesen, 2010). BA36 occupies the region from BA35 up to the fundus of the OTS; in higher resolution images, it is identifiable by a granular cell layer, though this is likely not visible in 3T images, and segmentation relies on the CS and OTS as landmarks. Thus, the first step to segmenting these structures is identifying these two sulci.

Collateral Sulcus (CS) and Occipito-Temporal Sulcus (OTS)

The CS also appears in two common patterns: a deep CS that is unbroken for the extent of the MTL (Type I), and a discontinuous CS (Type II) that has a distinct anterior and posterior component. Figures 16 and Figure 17 have examples of the different sulcal patterns. The OTS is identified as the sulcus lateral to CS. It was labeled as CSF in the previous segmentation protocol. Using a dedicated label for OTS rather than CSF is for the purpose of future development. Figures 16 and Figure 17 show two examples of OTS segmentations.

| ■ CA1 | ■ CA2 | ■ CA3 | ■ DG | ■ SUB | ■ CSF | ■ ERC | ■ BA35 | ■ BA36 | ■ CS | ■ OTS |
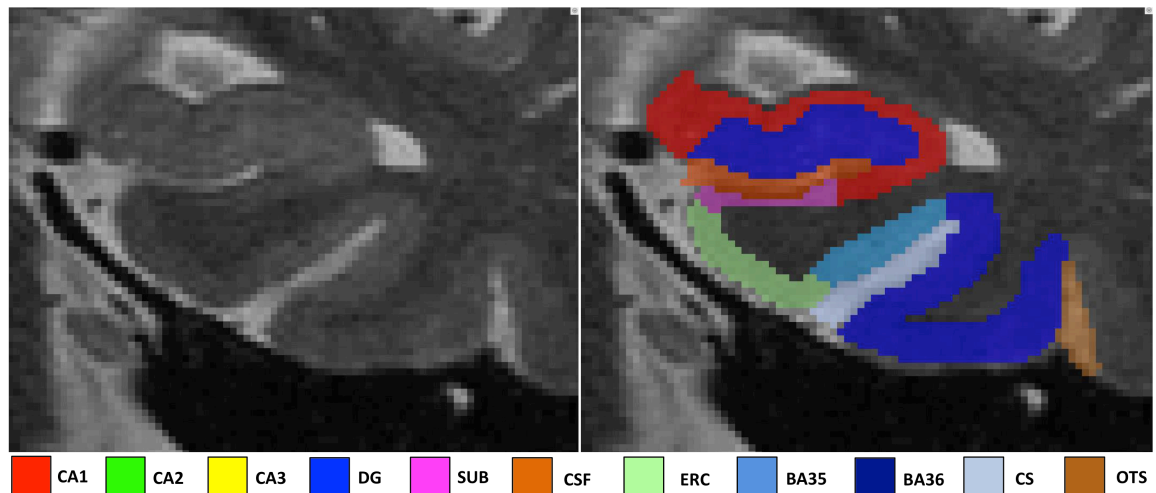
Figure 16. Type I collateral sulcus (CS) with segmentation. The Type I CS is deep and continuous along the anterior-posterior extent of PRC.
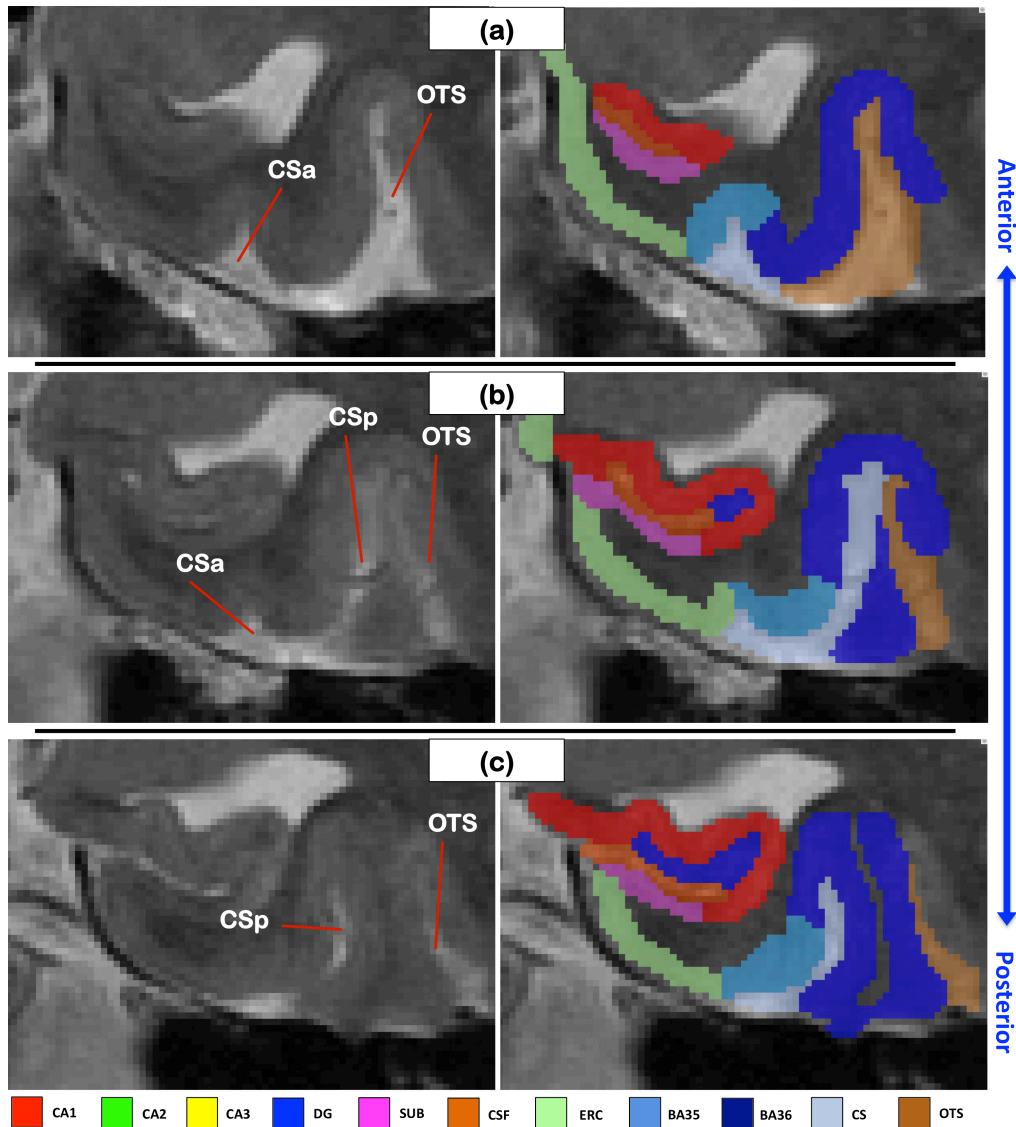
Figure 17. Type II collateral sulcus pattern with segmentation. The most anterior slice (a) contains the shallow anterior section of the sulcus (CSa). Moving in the posterior direction, the next slice (b) shows the transitional region between the two parts of the collateral sulcus, with a shallow anterior aspect (CSa) and a deep posterior (CSp). In the next slice (c), only a deep sulcus (CSp) is observed and CSa disappears. Blue arrow indicates the relative position of the three slices.

In general, in Type I cases BA35 is situated on the medial bank of the long CS, with BA36 continuing to the fundus of the OTS (Figure 16). In Type II cases, BA35 is the area over and around the shallow CS, with BA36 again terminating at the fundus of the OTS (Figure 17). The work in (Ding & Van Hoesen, 2010) provides detailed diagrams for each sulcal pattern, and once the pattern is identified, the figures in this paper are used to guide segmentation. Heuristic rules are not used except in difficult cases where the lateral extent of BA36 is unclear. It can be estimated as being 3-3.5 times longer than BA35 (Ding & Van Hoesen, 2010). The annotation tool can be used to measure length.

Parahippocampal Cortex (PHC)

The PHC is defined as the region posterior to PRC, and one slice anterior to the last slice of the hippocampal tail. This roughly corresponds to the area where the fusiform gyrus over takes PHC. The medial boundary is the SUB, and is identified by the greater thickness of PHC relative to SUB. The lateral boundary is the medial bank of the collateral sulcus, much like BA35. These boundaries are quite similar to the definitions in (Kivisaari et al., 2013) (Figure 18).
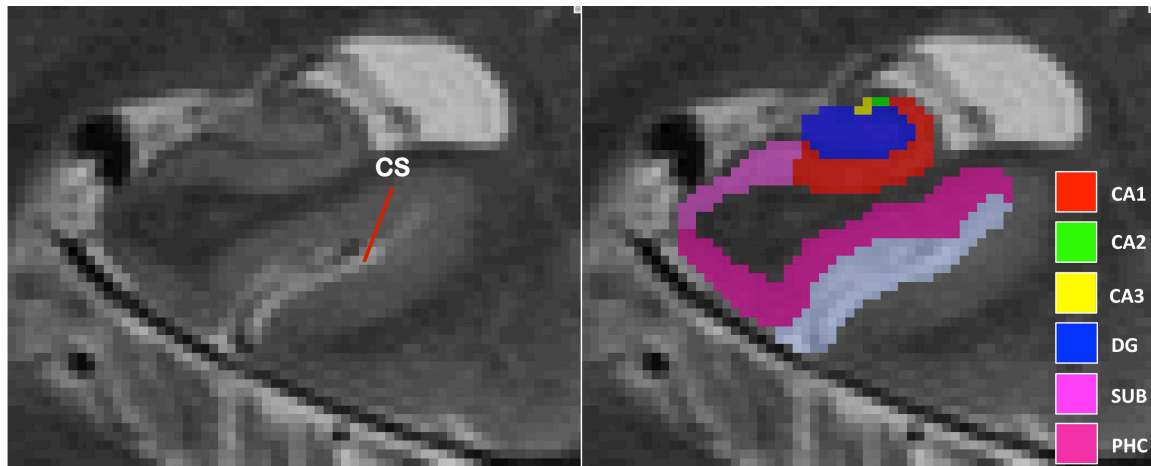
Figure 18. PHC begins posterior to PRC, and occupies the region between the SUB and the medial bank of the collateral sulcus.

References

Ding, S., Van Hoesen, G., Cassell, M., Poremba, A. 2009. Parcellation of human temporal polar cortex: A combined analysis of multiple cytoarchitectonic, chemoarchitectonic, and pathological markers. The Journal of Comparative Neurology, 514:595-623.

Ding, S., Van Hoesen, G. 2010. Borders, extent, and topography of human perirhinal cortex as revealed using multiple modern neuroanatomical and pathological markers. Human Brain Mapping, 31:1359-1379.

Duvernoy, H. 2005. The human hippocampus. Functional anatomy, vascularization and serial sections with MRI, Third edition. Springer. Verglag, Berlin.

Insausti, R., Juottonen, K., Soininen, H., Insausti, A., Partanen, K., Vainio, P., Laakso, M., Pitkanen, A. 1998. MR volumetric analysis of the human entorhinal, perirhinal, and temporopolar cortices. Am J Neuroradiol 19:659-671.

Kerchner, G., Hess, C., Hammond-Rosenbluth, K., Xu, D., Rabinovici, G, Kelley, D., Vigneron, D., Nelson, S., Miller, B. 2010. Hippocampal CA1 apical neuropil atrophy in mild Alzheimer disease visualized with 7-T MRI. Neurology 75(15):1381-7.

Kivisaari, S., Probst, A., Taylor, K. 2013. The peririhnal, entorhinal, parahippocampal cortices and hippocampus: An overview of functional anatomy and protocol for their segmentation in MR images. fMRI – basices and clinical applications. Springer-Verlag, Berlin, Germany.

Malykhin, N., Lebel, R., Coupland, N., Wilman, A., Carter, R. 2010. In vivo quantification of hippocampal subfields using 4.7T fast spin echo imaging. NeuroImage 49(2):1224-1230.

Mueller, S.G., Stables, L., Du, A.T., Schuff, N., Truran, D., Cashdollar, N., Weiner, M. 2007. Measurements of hippocampal subfields and age related changes with high resolution MRI at 4T. Neurobiol Aging 28(5):719-726.

Wisse, L., Gerritsen, L., Zwanenburg, J., Kujif, H., Luijten, P., Biessels, G., Geerlings, M. 2012. Subfields of the hippocampal formation at 7T MRI: In vivo volumetric assessment. NeuroImage 61:1043-1049.

Yushkevich, P., Avants, B., Pluta, J., Das, S., Minkoff, D., Mechanic-Hamilton, D., Glynn, S., Pickup, S., Liu, W., Gee, J., Grossman, M., Detre, J. 2009. A high-resolution computational atlas of the human hippocampus from postmortem magnetic resonance imaging at 9.4T. NeuroImage 44:385-398.

Yushkevich, P., Piven, J., Cody Hazlett, H., Gimpel Smith, R., Ho, S., Gee, J., Gerig, Guido. 2006. User-guided 3D active contour segmentation of anatomical structures: Significantly improved efficiency and reliability. NeuroImage 31(3):1116-28.

Yushkevich, P., Wang, H., Pluta, J., Das, S., Craige, C., Avants, B., Weiner, M., Mueller, S. 2010. Nearly automatic segmentation of hippocampal subfields in in vivo focal T2-weighted MRI. NeuroImage 53(4):1208-24.

Yushkevich P., Pluta J., Wang H., Xie L., Ding S., Gertje G., Mancuso L., Kliot D., Das S., Wolk D. 2014. Automated volumetry and regional thickness analysis of hippocampal subfields and medial temporal cortical structures in mild cognitive impairment. Hum Brain Mapp 36:258–287.